The RING-finger domain of *Arabidopsis* RMR functions as an E3 ligase essential for post-Golgi trafficking

Shuai Chen,[a,1] Yonglun Zeng, [b,1] Hiu Yan Wong,[a,1] Yihong Chen,[a] Lei Yang,[a] Fang Luo,[c] Caiji Gao,[d] Liwen Jiang,[b]* Kam-Bo Wong [a]*

[a] Centre for Protein Science and Crystallography, [b] Centre for Cell and Developmental Biology, State Key Laboratory of Agrobiotechnology, School of Life Sciences, The Chinese University of Hong Kong, Shatin, Hong Kong, China

[c] Department of Developmental Biology, School of Basic Medical Sciences, Southern Medical University, Guangzhou, Guangdong 510515, China

[d] Guangdong Provincial Key Laboratory of Biotechnology for Plant Development, School of Life Sciences, South China Normal University, Guangzhou 510631, China

[1] These authors contributed equally to this article.

* To whom correspondence should be addressed.

Email:

Liwen Jiang ljiang@cuhk.edu.hk;

Kam-Bo Wong: kbwong@cuhk.edu.hk

Running title: E3 Ligase Activity of RMR in Post-Golgi Trafficking

Abstract

Receptor-homology-transmembrane-RING-H2 (RMR) sorting receptors are essential for directing soluble cargo proteins to protein storage vacuoles in plants. These type I integral membrane proteins comprise a single transmembrane domain, an N-terminal lumenal region containing a protease-associated domain for cargo recognition, and a C-terminal cytoplasmic region (CT) with a Really-Interesting-New-Gene-H2 (RING-H2) domain. Here, we determined the crystal structure of the RING-H2 domain of *Arabidopsis* RMR isoform-1 (AtRMR1-RING), where the conserved C3H2C3 motif coordinates two Zn ions, a feature typical of RING-type E3 ligases. AtRMR1-RING was shown to interact with *Arabidopsis* E2 ubiquitin-conjugating enzyme, and exhibits E3 ligase activity in an in vitro ubiquitination assay. Biochemical analysis reveals that I234Y substitution disrupted the E2/E3 interaction and greatly reduced E3 ligase activity. Furthermore, we showed that the conserved RING-H2 domains of AtRMR isoform 2, 3 and 4 are also E3 ligases. Inactivation of E3 ligase activity by the I234Y mutation resulted in Golgi retention of AtRMR1-CT and AtRMR2. These findings suggest that the E3 ligase activity is essential for post-Golgi trafficking of RMR receptors, providing new insights into receptor-mediated protein sorting in plants.

Key words: RMR, RING structure, protein trafficking, E3 ligase, ubiquitination

Introduction

Plant cells are characterized by a prominent vacuolar system, which occupies a significant portion of the cell volume (1). This system consists primarily of two types of vacuoles: lytic vacuoles and protein storage vacuoles (PSVs). Lytic vacuoles play roles in various cellular processes, including metabolites recycling, defence against infection, autophagy and programmed cell deaths (2). In contrast, PSVs are responsible for the accumulation of storage proteins in developing seeds. A key mechanism by which soluble cargo proteins are sorted to plant vacuoles involves the action of sorting receptors (3). Specifically, the sorting of soluble cargo proteins to vacuoles is mediated by type I transmembrane receptors, namely vacuolar sorting receptors (VSR) and receptor-homology-transmembrane-RING-H2 (RMR) proteins (4). Both receptor families share common structural features, including an N-terminal lumenal region (NT) responsible for cargo binding, and C-terminal cytoplasmic regions (CT) that are crucial for targeting and subcellular localization (5-12).

RMR contains a protease-associated (PA) domain in the NT, separated by a transmembrane domain (TMD), and a Really-Interesting-New-Gene-H2 (RING-H2) domain in the CT (Fig. 1A). The PA domain, responsible for receptor-cargo interactions, is present in both VSR and RMR (5, 7, 9, 10, 12, 13), whereas the CT of these receptors differ markedly. VSR contains a short cytosolic tail with the conserved YxxΦ and acidic dileucine-like motifs that determine its trafficking (3, 14), whereas RMR has a distinct C-terminal RING-H2 domain (11, 15) (Fig. 1A). Early studies revealed that the NT of RMR is responsible for directing the reporter protein pro-aleurain to storage vacuoles via the Golgi apparatus (6). In contrast, fusion of RMR's NT with TMD and CT of VSR resulted in the mislocalization of the fusion product to lytic vacuoles (16). These findings suggest that RMR and VSR follow distinct trafficking pathways, with the CT of RMR playing a crucial role in the proper targeting and transport of cargo to its correct destination.

Despite these insights, the biological function of the C-terminal RING-H2 domain of RMR remains poorly understood. Interestingly, this domain is also present in other mammalian E3 ligases known to be involved in protein trafficking (17). In this study, we determined the crystal structure of the RING-H2 domain of Arabidopsis RMR isoform 1 (AtRMR1-RING), revealing its structural similarity to known E3 ligases. Our

in vitro studies further confirm that the RING-H2 domain of AtRMR1-4 functions as an E3 ligase. Additionally, we show that I234Y substitution, which disrupts E3 ligase activity, results in the retention of RMR in the Golgi apparatus of *Arabidopsis* protoplasts, highlighting the essential role of ubiquitination in protein trafficking.

Results

Crystal structure of AtRMR1-RING

RMR sorting receptors are type-1 transmembrane protein that adopt a PA-TMD-RING domain organization, with a protease-associated (PA) domain at the N-terminal region (NT), a transmembrane domain (TMD), and a RING-H2 domain at the C-terminal region (CT) (Fig. 1A). To better understand how the CT of RMR affects protein trafficking, we determined the crystal structure of the RING-H2 domain of AtRMR1 (AtRMR1-RING, residue 206-283) to a resolution of 2.1 Å (Fig. 1B and Table S1). There are two AtRMR1-RING in the crystallographic asymmetric unit (Fig. S1A) and each AtRMR1-RING binds two zinc ions by the C3H2C3 motif – the first zinc ion is coordinated in a tetrahedral geometry by the $_{232}$CxxC$_{235}$ and $_{252}$HxxC$_{255}$ motifs, while the second one by the $_{250}$CxH$_{252}$ and $_{270}$CxxC$_{273}$ motifs (Fig. S1B). The C3H2C3 motif is conserved in the RING-H2 domain of other known E3 ligases with the same PA-TMD-RING topology (Fig. S1C).

We further compared the crystal structure of AtRMR1-RING with other known crystal structures of RING-H2 domain from RNF13, RNF38 (18), and RNF165 (19) (Fig. 1C and 1D). The structure of AtRMR1-RING is similar to other RING-H2 domains, adopting the typical RING finger fold (20). However, helix-2 of AtRMR1-RING is not found in RNF13 and RNF38, while the corresponding residues in RNF165 are disordered.

AtRMR1-RING is an E3 ligase

Given that the sequence and structure of AtRMR1-RING resemble those of known E3 ligases, it is likely that AtRMR1-RING is also an E3 ligase. As glutathione-S-transferase (GST) has been previously shown to serve as a substrate for E3 ligase in an auto-ubiquitination assay (21), we tested if AtRMR1-RING is an E3 ligase by mixing GST-tagged AtRMR1-RING (GST-AtRMR1-RING) with *Arabidopsis* E1 ubiquitin-activating enzyme (AtUba1, At2g30110), E2 ubiquitin-conjugating enzyme (AtUbc30, At5g56150) and ubiquitin (AtUb, At4g02890) in the presence of Mg^{2+} and ATP. In the presence of both E1 and E2 enzymes, poly-ubiquitination was detected

in GST-AtRMR1-RING but not in the GST control (Fig. 2A), suggesting that AtRMR1-RING is indeed an E3 ligase.

I234Y substitution greatly reduced the E3 ligase activity of AtRMR1-RING

To further understand how AtRMR1-RING interacts with its E2 ubiquitin-conjugating enzyme, we modelled the complex structure of AtRMR1-RING/AtUbc30 based on the complex structure of RNF38/UbcH5B/ubiquitin (18) (Fig. S2). The model suggests that Ile234 of AtRMR1 undergoes hydrophobic interactions with the E2 ubiquitin-conjugating enzyme (Fig. 2B). Interestingly, Ile234 is highly conserved and this residue has been shown to be crucial for the activity of other RING E3 ligases (22, 23).

To test the role of Ile234 in AtRMR1, we created an I234Y variant of AtRMR1-RING and tested its ability to form a E2/E3 complex via a GST pull-down assay (Fig. 2C). Substitution of a bulky tyrosine residue was expected to break the E2/E3 interaction by creating steric clashes in the interface (Fig. 2B). Our results showed that while wild-type GST-AtRMR1-RING can interact with AtUbc30, the I234Y substitution abolished the interaction between AtRMR1-RING and AtUbc30 (Fig. 2C). As RING-type E3 ligases promote catalysis by forming an E2/E3 complex so that the substrate is juxtaposed to the E2-ubiquitin thioester (24), we expected that the I234Y substitution should inactivate the E3 ligase activity of AtRMR1-RING. To test this hypothesis, we performed the *in vitro* ubiquitination assay and showed that I234Y substitution did indeed greatly reduced the E3 ligase activity of AtRMR1-RING (Fig. 2D).

E3 ligase activity of AtRMR1 is essential for its protein trafficking

To further investigate the *bona fide* function of AtRMR1-RING as an E3 ligase and its impacts on protein trafficking, we performed an *in vivo* analysis using our established *Arabidopsis* protoplast transient expression system (25). It has been shown that the CT is involved in targeting individual VSRs and RMRs to their final

destinations (6-8), we thus used similar strategies to study the localization of AtRMR1 as well as the I234Y mutant. GFP-TMD-AtRMR1-CT exhibited partial colocalization with both the Golgi marker (ManI-RFP) and *trans*-Golgi-network (TGN) marker (mRFP-SYP61) (Fig. 3A). Strikingly, the I234Y mutant of AtRMR1 (GFP-TMD-AtRMR1-CT-I234Y) colocalized substantially with the Golgi marker but not the TGN marker (Fig. 3B), suggesting that the I234Y substitution resulted in retention of the protein in the Golgi apparatus.

The RING domains of AtRMR2-4 are also E3 ligases

Given that AtRMR1-RING functions as an E3 ligase and the RING-H2 domain is conserved across AtRMR homologs (Fig. 4A), we hypothesized that they might exhibit similar E3 ligase activity. To address this hypothesis, we tagged GST to the N-termini of the RING-H2 domain of AtRMR2-4 and tested their E3 ligase activity (Fig. 4B-D). In the presence of both E1 and E2 enzymes, polyubiquitination was detected in GST-AtRMR2-4-RING. On the other hand, no poly-ubiquitination was observed when either E1 or E2 enzymes were omitted in the reaction buffer or in the GST control. These observations suggest that the RING-H2 domain of AtRMR2-4 are E3 ligases.

I234Y substitution led to Golgi retention of AtRMR2

Similar to AtRMR1, AtRMR2 also contains the conserved Ile234 residue in its RING-H2 domain (Fig. 4A). We also show that the I234Y substitution abolished the E3 ligase activity of AtRMR2-RING (Fig. 4B). Next, we investigated if the I234Y mutation affects the trafficking of AtRMR2. Consistent with previous results (11), GFP-AtRMR2 partially co-localized with the Golgi and TGN markers (Fig. 5A). On the other hand, the I234Y mutation resulted in increased retention of GFP-AtRMR2 in the Golgi apparatus (Fig. 5). These findings suggest that inactivation of the E3 ligase activity by the I234Y substitution leads to retention of both GFP-TMD-AtRMR1-CT and GFP-AtRMR2 in the Golgi (Fig. 3 and 5), further supporting the conclusion that E3 ligase activity of the CT of RMR receptors is essential for their proper post-Golgi trafficking.

Discussion

One prominent feature of RMR is the presence of a conserved RING-H2 domain in the CT. While the CT of RMR has been implicated in protein targeting (6, 7, 9, 11), the underlying mechanism remains elusive. Due to its sequence similarity to other well-characterized RING-type E3 ligases (Fig. S1), the role of RMR proteins as E3 ligases has long been hypothesized (15). Here, we present the crystal structure of the RING-H2 domain of AtRMR1 (Fig. 1) and showed that the RING-H2 domains of AtRMR1-4 are E3 ligases (Fig. 2 and 4). We further showed that the I234Y mutation that disturbing the E3 ligase activity resulted in Golgi retention of GFP-TMD-AtRMR1-RING and GFP-AtRMR2 in *Arabidopsis* protoplasts (Fig. 3 and 5). Our observation is consistent with a pioneer study of Park and co-workers, who showed that truncation of the CT of AtRMR1 resulted in its co-localization with the Golgi apparatus and blocked its trafficking to DIP organelles in *Arabidopsis* protoplasts (7). It is tempting to speculate that the E3 ligase activity of RMR provide a novel mechanism to regulate its post-Golgi trafficking such that disturbing the poly-ubiquitination by I234Y substitution resulted in aberrant accumulation of RMR in the Golgi apparatus.

It has been well established that ubiquitination plays an essential role in the endocytic pathway and in protein degradation to lysosomes/vacuoles (26-29). In yeast and mammalian cells, GGA (Golgi-localized, γ-adaptin ear-containing, ADP ribosylation factor-binding protein) serves as an Endosomal-Sorting-Complex-Required-for-Transport (ESCRT)-0-like component to convey ubiquitinated cargos to the lysosomal degradation (29-31). Although GGA is absent in plants, its role is likely replaced by a related TOL (Tom-1 Like) protein, which also contains the conserved VHS and GAT domains for cargo recognition (27). For example, *Arabidopsis* TOL2 and TOL6 serve as receptors for ubiquitinated proteins and are involved in the vacuolar degradation of plasma membrane proteins via the ESCRT pathway (32, 33). In a recent study, Xu and co-workers showed that recognition of the ubiquitination on

Snc1, a SNARE protein, by the WD40 domain of COPI coatomers is essential for the recycling of Snc1 in yeast (34). They argued that poly-ubiquitination provides a COPI-dependent sorting signal that redirects cargos from the endocytic pathway to the TGN and is independent to the known COPI-mediated retrograde transport of cargos from the Golgi apparatus to the ER (34). It is possible that E3 ligase activity is required for post-Golgi trafficking of RMR so that mutations abolishing E3 ligase activity block post-Golgi trafficking of AtRMR1 and result in retention of the mutated proteins in the Golgi. A similar scenario was reported for RNF11 (ring finger protein 11), a RING-H2 E3 ligase that drives the ubiquitination of GGA3 and governs RNF11 sorting at the TGN, in mammalian cells (35). Accordingly, a lysine-less mutant of RNF11, which cannot be ubiquitinated, was found to accumulate in the Golgi (36).

In developing seeds, RMR is targeted to the protein storage vacuoles (PSV) (6, 15, 37). The presence of complex glycans in RMR strongly suggests its trafficking through the Golgi (6). RMR was also found in dense vesicles (DV) and in the storage pre-vacuolar compartments (PVC) or DIP organelles (7, 38, 39). In a working model for RMR trafficking, it has been proposed that RMR is involved in the aggregation of storage proteins from the Golgi into dense vesicles, which are then internalized into storage PVC during their passage to the PSV (15). Given that ubiquitin was also found in the PSV (15) and the RING-H2 domain is only found in RMR but not in VSR, it would be tempting to speculate that ubiquitination of RMR may provide a plausible mechanism to regulate sorting of storage proteins to the PSV, thus separating them from VSR-mediated sorting of cargos to the lytic vacuoles.

Experimental procedures

Plasmid construction

To create vectors for protein expression in *E. coli*, codon-optimized coding sequences of AtRMR1-RING (206-283), AtRMR1-CT (191-310), AtUba1 (72-1080), AtUbc30, AtUb were ordered from GenScript (http://www.genscript.com), AtRMR2-RING (207-283), AtRMR3-RING (207-282), AtRMR4-RING (209-284) were PCR amplified and all cloned into the pGEX-6p-1 vector (for GST-tagged fusion proteins) or pRSETA-His vector (for polyhistidine-small-ubiquitin-like-modifier(SUMO)-tagged fusion protein) as listed in the Table S2. To create GFP-tagged constructs for

transient expression in *Arabidopsis* protoplasts, coding sequences of AtRMR1-CT (160-310), AtRMR1 (28-310) and AtRMR2 (22-448) were cloned into pBI221 to create GFP-TMD-AtRMR1-CT, GFP-AtRMR1 and GFP-AtRMR2, respectively (Table S2). I234Y mutation was introduced using Q5 site-directed mutagenesis kit (New England BioLabs) with primers listed in Table S3.

Protein Expression and Purification of AtRMR1-RING, AtUba1, AtUbc30 and AtUb

Expression vectors pGEX-6p-1-AtRMR1-4-RING, pGEX-6p-1AtUba1, pGEX-6p-1-AtUbc30 and pGEX-6p-1-AtUb were transformed into *E. coli* SoluBL21 cell (Genlantis). Protein expression was induced by 0.4 mM isopropyl beta-D-1-thiogalactopyranoside (IPTG) at OD_{600} 0.8. After incubation at 16 ℃ for 18 h, the cells were harvested by centrifugation at 14,160g for 12 min. The cell pellet was resuspended in the 30 mM Tris buffer pH 7.6, 500 mM NaCl, 5 μM $ZnCl_2$ and 5 mM dithiothreitol (DTT) and sonicated on ice. After centrifugation at 29,000×g for 36 min, the supernatant was filtered and then incubated with GSTrap Sepharose (GE Healthcare) for 2 h at 4 ℃. After extensive washing with 30 mM Tris, pH 7.6, 150 mM NaCl and 5 mM DTT, GST-tagged PreScission protease (GE Healthcare) was added to remove the GST tag by incubation at 4 ℃ overnight. The target proteins were then collected in the unbound fractions, and further purified by gel filtration using a HiLoad 26/60 Superdex 75 column (GE Healthcare) pre-equilibrated with 30 mM Tris, pH 7.5, 150 mM NaCl, 5 μM $ZnCl_2$ and 2 mM DTT.

Crystallization and Structure Determination

Crystals of AtRMR1-RING were obtained using hanging-drop-vapour-diffusion by mixing 1 μl protein solution (15 mg/ml in 30 mM Tris, pH 7.5, 150 mM NaCl, 5 μM $ZnCl_2$ and 2 mM DTT) with 1 μl reservoir solution containing 0.2 M ammonium acetate, 0.1 M Bis-Tris pH 5.5, 20% w/v polyethylene glycol 3,350 at 16 ℃. Cryoprotection was achieved with 15% glycerol. Diffraction data were collected using an in-house rotating anode X-ray generator (Rigaku FR-E+), and processed with the XDS package (40) and the CCP4 program suite (41). The phase was solved by molecular replacement using the program MOLREP (42) with the crystal structure of RNF38 (PDB:4V3K) as the search template. Models were built interactively using the

program COOT (43) and refined using the program PHENIX (44). All molecular graphics in the manuscript were generated with PyMOL (http://www.pymol.org).

Modelling of AtRMR1-RING/AtUbc30 complex structure

The structure of AtUbc30 was predicted by homology modeling using the crystal structure of the human RNF38/UbcH5B complex (PDB: 4V3K) as the template. Sequences of AtUbc30 and UbcH5B were aligned using the program ClustalW (45) and edited using the program CHIMERA (46). Structure models of AtRMR1-RING in complex with AtUbc30 were generated using the program MODELLER as described (47, 48).

Pull down assay

50-60 μM purified AtUbc30 was incubated with equimolar of GST, wild-type or I234Y variant of GST-AtRMR1-RING in the presence of GSTrap Sepharose (GE Healthcare) in a binding buffer (30 mM Tris, pH 7.5, 150 mM NaCl and 2 mM DTT) for 4 h at 4 ℃. After extensive washing with the binding buffer, bound proteins were eluted with 20 mM reduced glutathione in the binding buffer.

Ubiquitination assay

Ubiquitination assay reaction was performed in a 30 μl reaction mixture by incubating 1 μg recombinant GST-AtRMR1-RING (as in Fig. 2), GST-AtRMR2-RING (as in Fig. 4), GST-AtRMR3-RING (as in Fig. S4A) or GST-AtRMR4-RING (as in Fig. S4B) with 0.1 μg AtUba1, 0.3 μg AtUbc30, 2.5 μg AtUb in a reaction buffer (30 mM Tris-HCl, pH 7.5, 2 mM ATP, 5 mM $MgCl_2$, 2 mM DTT and 0.5 U inorganic pyrophosphatase (Sigma)). The reaction mixture was incubated at 30 ℃ for 30 min, and then analyzed by SDS-PAGE using 4–12% gradient gel (Bolt Bis-Tris Plus Gel, Thermo Fisher Scientific) and detected by Western blot using ubiquitin (FK2, ENZO), GST (Abcam) or AtRMR1-RING antibodies.

Protoplast transient expression assay

Transient expression in *Arabidopsis* PSBD protoplasts was performed as described previously (8). Transfected protoplasts were incubated for 12–16 h before confocal imaging using Leica SP8.

Accession numbers

The crystal structure of AtRMR1-RING was deposited in the Protein Data Bank (PDB codes: 7BVW). *Arabidopsis* sequences used in this study can be found with the following accession numbers: RMR1, At5g66160; RMR2, At1g71980; RMR3, At1g22670; RMR4, At4g09560; Uba1, At2g30110; Ubc30, At5g56150; ubiquitin, At4g02890.

Author contributions

S. C. & **Y. L.**: writing – original draft, review & editing; conceptualization, visualization, resources, investigation, formal analysis. **H. Y. W.:** conceptualization, visualization, investigation, validation, formal analysis, writing – review & editing. **Y. C., L. Y., F. L. and C. J. G.:** investigation. **L. J.,** & **K. B. W.:** supervision, project administration, resources, conceptualization, visualization, funding acquisition, writing – original draft, review & editing.

Acknowledgements

This study was supported by grants from the Research Grants Council of Hong Kong SAR (CUHK14151416, CUHK14118122, C4002-17GF, C4041-18EF, AoE/M-05/12, AoE/M403/16, C4012-16E, C4033-19E, and C2003-22W), NSFC (91854201 and 31670179) and Direct Grants from the Chinese University of Hong Kong.

Conflict of interest

The authors declare that they have no conflicts of interest with the contents of this article.

References

1. Zouhar, J., and Rojo, E. (2009) Plant vacuoles: where did they come from and where are they heading? *Curr. Opin. Plant Biol.* **12**, 677-684.
2. Shimada, T., Takagi, J., Ichino, T., Shirakawa, M., and Hara-Nishimura, I. (2018) Plant vacuoles. *Annu. Rev. Plant Biol.* **69**, 123-145.
3. Robinson, D. G., and Neuhaus, J.-M. (2016) Receptor-mediated sorting of soluble vacuolar proteins: myths, facts, and a new model. *J. Exp. Bot.* **67**, 4435-4449.
4. De Marcos Lousa, C., Gershlick, D. C., and Denecke, J. (2012) Mechanisms and concepts paving the way towards a complete transport cycle of plant vacuolar sorting receptors *The Plant Cell* **24**, 1714-1732.

5. Cao, X., Rogers, S. W., Butler, J., Beevers, L., and Rogers, J. C. (2000) Structural requirements for ligand binding by a probable plant vacuolar sorting receptor. *Plant Cell* **12**, 493-506.
6. Jiang, L., Phillips, T. E., Rogers, S. W., and Rogers, J. C. (2000) Biogenesis of the protein storage vacuole crystalloid. *J. Cell Biol.* **150**, 755-770.
7. Park, M., Lee, D., Lee, G.-J., and Hwang, I. (2005) AtRMR1 functions as a cargo receptor for protein trafficking to the protein storage vacuole. *J. Cell Biol.* **170**, 757-767.
8. Miao, Y., Yan, P. K., Kim, H., Hwang, I., and Jiang, L. (2006) Localization of green fluorescent protein fusions with the seven Arabidopsis vacuolar sorting receptors to prevacuolar compartments in tobacco BY-2 cells. *Plant Physiol.* **142**, 945-962.
9. Park, J. H., Oufattole, M., and Rogers, J. C. (2007) Golgi-mediated vacuolar sorting in plant cells: RMR proteins are sorting receptors for the protein aggregation/membrane internalization pathway. *Plant Sci.* **172**, 728-745.
10. Luo, F., Fong, Y. H., Zeng, Y., Shen, J., Jiang, L., and Wong, K.-B. (2014) How vacuolar sorting receptor proteins interact with their cargo proteins: crystal structures of apo and cargo-bound forms of the protease-associated domain from an Arabidopsis vacuolar sorting receptor. *Plant Cell* **26**, 3693-3708.
11. Occhialini, A., Gouzerh, G., Di Sansebastiano, G.-P., and Neuhaus, J.-M. (2016) Dimerization of the vacuolar receptors AtRMR1 and-2 from Arabidopsis thaliana contributes to their localization in the trans-Golgi network. *Int. J. Mol. Sci.* **17**, 1661.
12. Tsao, H.-E., Lui, S. N., Lo, A. H.-F., Chen, S., Wong, H. Y., Wong, C.-K. *et al.* (2022) Structural insights into how vacuolar sorting receptors recognize the sorting determinants of seed storage proteins. *Proc. Natl. Acad. Sci.* **119**, e2111281119.
13. Mahon, P., and Bateman, A. (2000) The PA domain: a protease-associated domain. *Protein Sci.* **9**, 1930-1934.
14. de Marcos Lousa, C., and Denecke, J. (2016) Lysosomal and vacuolar sorting: not so different after all! *Biochemical Society Transactions* **44**, 891-897.
15. Wang, H., Rogers, J. C., and Jiang, L. (2011) Plant RMR proteins: unique vacuolar sorting receptors that couple ligand sorting with membrane internalization. *FEBS J.* **278**, 59-68.
16. Jiang, L., and Rogers, J. C. (1998) Integral membrane protein sorting to vacuoles in plant cells: evidence for two pathways. *J. Cell Biol.* **143**, 1183-1199.
17. Yamazaki, Y., Schönherr, C., Varshney, G. K., Dogru, M., Hallberg, B., and Palmer, R. H. (2013) Goliath family E3 ligases regulate the recycling endosome pathway via VAMP3 ubiquitylation. *EMBO J.* **32**, 524-537.
18. Buetow, L., Gabrielsen, M., Anthony, N. G., Dou, H., Patel, A., Aitkenhead, H. *et al.* (2015) Activation of a primed RING E3-E2–ubiquitin complex by non-covalent ubiquitin. *Mol. Cell* **58**, 297-310.
19. Wright, J. D., Mace, P. D., and Day, C. L. (2016) Secondary ubiquitin-RING docking enhances Arkadia and Ark2C E3 ligase activity. *Nat. Struct. Mol. Biol.* **23**, 45-52.
20. Zhang, X., Chen, J., Wu, M., Wu, H., Arokiaraj, A. W., Wang, C. *et al.* (2013) Structural basis for role of ring finger protein RNF168 RING domain. *Cell Cycle* **12**, 312-321.
21. Nian, H., Zhang, W., Shi, H., Zhao, Q., Xie, Q., Liao, S. *et al.* (2008) Mouse RING finger protein Rnf133 is a testis-specific endoplasmic reticulum-associated E3 ubiquitin ligase. *Cell Res.* **18**, 800-802.

22. Deshaies, R. J., and Joazeiro, C. A. (2009) RING domain E3 ubiquitin ligases. *Annu. Rev. Biochem.* **78**, 399-434.
23. Yuan, L., Lv, Z., Atkison, J. H., and Olsen, S. K. (2017) Structural insights into the mechanism and E2 specificity of the RBR E3 ubiquitin ligase HHARI. *Nat. Commun.* **8**, 211.
24. Buetow, L., and Huang, D. T. (2016) Structural insights into the catalysis and regulation of E3 ubiquitin ligases. *Nat. Rev. Mol. Cell Biol.* **17**, 626-642.
25. Miao, Y., and Jiang, L. (2007) Transient expression of fluorescent fusion proteins in protoplasts of suspension cultured cells. *Nat. Protoc.* **2**, 2348-2353.
26. Clague, M. J., Liu, H., and Urbé, S. (2012) Governance of endocytic trafficking and signaling by reversible ubiquitylation. *Dev. Cell* **23**, 457-467.
27. Gao, C., Zhuang, X., Shen, J., and Jiang, L. (2017) Plant ESCRT complexes: moving beyond endosomal sorting. *Trends Plant Sci.* **22**, 986-998.
28. Uemura, T., and Waguri, S. (2020) Emerging roles of Golgi/endosome-localizing monomeric clathrin adaptors GGAs. *Anat. Sci. Int.* **95**, 12-21.
29. Puertollano, R., and Bonifacino, J. S. (2004) Interactions of GGA3 with the ubiquitin sorting machinery. *Nat. Cell Biol.* **6**, 244-251.
30. Kang, E. L., Cameron, A. N., Piazza, F., Walker, K. R., and Tesco, G. (2010) Ubiquitin regulates GGA3-mediated degradation of BACE1 *Journal of Biological Chemistry* **285**, 24108-24119.
31. Shiba, Y., Katoh, Y., Shiba, T., Yoshino, K., Takatsu, H., Kobayashi, H. *et al.* (2004) GAT (GGA and Tom1) domain responsible for ubiquitin binding and ubiquitination. *J. Biol. Chem.* **279**, 7105-7111.
32. Korbei, B., Moulinier-Anzola, J., De-Araujo, L., Lucyshyn, D., Retzer, K., Khan, M. A. *et al.* (2013) Arabidopsis TOL proteins act as gatekeepers for vacuolar sorting of PIN2 plasma membrane protein. *Curr. Biol.* **23**, 2500-2505.
33. Moulinier-Anzola, J., Schwihla, M., De-Araújo, L., Artner, C., Jörg, L., Konstantinova, N. *et al.* (2020) TOLs function as ubiquitin receptors in the early steps of the ESCRT pathway in higher plants. *Mol. Plant* **13**, 717-731.
34. Xu, P., Hankins, H. M., MacDonald, C., Erlinger, S. J., Frazier, M. N., Diab, N. S. *et al.* (2017) COPI mediates recycling of an exocytic SNARE by recognition of a ubiquitin sorting signal. *elife* **6**, e28342.
35. Santonico, E., Mattioni, A., Panni, S., Belleudi, F., Mattei, M., Torrisi, M. R. *et al.* (2015) RNF11 is a GGA protein cargo and acts as a molecular adaptor for GGA3 ubiquitination mediated by Itch *Oncogene* **34**, 3377-3390.
36. Malonis, R. J., Fu, W., Jelcic, M. J., Thompson, M., Canter, B. S., Tsikitis, M. *et al.* (2017) RNF11 sequestration of the E3 ligase SMURF2 on membranes antagonizes SMAD7 down-regulation of transforming growth factor β signaling. *J. Biol. Chem.* **292**, 7435-7451.
37. Gillespie, J., Rogers, S. W., Deery, M., Dupree, P., and Rogers, J. C. (2005) A unique family of proteins associated with internalized membranes in protein storage vacuoles of the Brassicaceae. *Plant J.* **41**, 429-441.
38. Hinz, G., Colanesi, S., Hillmer, S., Rogers, J. C., and Robinson, D. G. (2007) Localization of vacuolar transport receptors and cargo proteins in the Golgi apparatus of developing Arabidopsis embryos. *Traffic* **8**, 1452-1464.

39. Shen, Y., Wang, J., Ding, Y., Lo, S. W., Gouzerh, G., Neuhaus, J.-M. *et al.* (2011) The rice RMR1 associates with a distinct prevacuolar compartment for the protein storage vacuole pathway. *Mol. Plant* **4**, 854-868.
40. Kabsch, W. (2010) xds. *Acta Crystallogr. Sect. D Biol. Crystallogr.* **66**, 125-132.
41. Winn, M. D., Ballard, C. C., Cowtan, K. D., Dodson, E. J., Emsley, P., Evans, P. R. *et al.* (2011) Overview of the CCP4 suite and current developments. *Acta Crystallogr. Sect. D Biol. Crystallogr.* **67**, 235-242.
42. Vagin, A., and Teplyakov, A. (2010) Molecular replacement with MOLREP. *Acta Crystallogr. Sect. D Biol. Crystallogr.* **66**, 22-25.
43. Emsley, P., and Cowtan, K. (2004) Coot: model-building tools for molecular graphics. *Acta Crystallogr. Sect. D Biol. Crystallogr.* **60**, 2126-2132.
44. Adams, P. D., Afonine, P. V., Bunkóczi, G., Chen, V. B., Davis, I. W., Echols, N. *et al.* (2010) PHENIX: a comprehensive Python-based system for macromolecular structure solution. *Acta Crystallogr. Sect. D Biol. Crystallogr.* **66**, 213-221.
45. Thompson, J. D., Higgins, D. G., and Gibson, T. J. (1994) CLUSTAL W: improving the sensitivity of progressive multiple sequence alignment through sequence weighting, position-specific gap penalties and weight matrix choice. *Nucleic Acids Res.* **22**, 4673-4680.
46. Pettersen, E. F., Goddard, T. D., Huang, C. C., Couch, G. S., Greenblatt, D. M., Meng, E. C. *et al.* (2004) UCSF Chimera—a visualization system for exploratory research and analysis. *J. Comput. Chem.* **25**, 1605-1612.
47. Fiser, A., and Šali, A. (2003) Modeller: generation and refinement of homology-based protein structure models. In *Methods Enzymol.*, Elsevier, 461-491.
48. Nim, Y.-S., Sun, S., and Wong, K.-B. (2017) Using homology modeling to understand the structural basis of specific interaction of a plant-specific AtSar1a–AtSec23a pair involved in protein ER export. In *Plant Protein Secretion: Methods and Protocols*, 59-73.

Figures

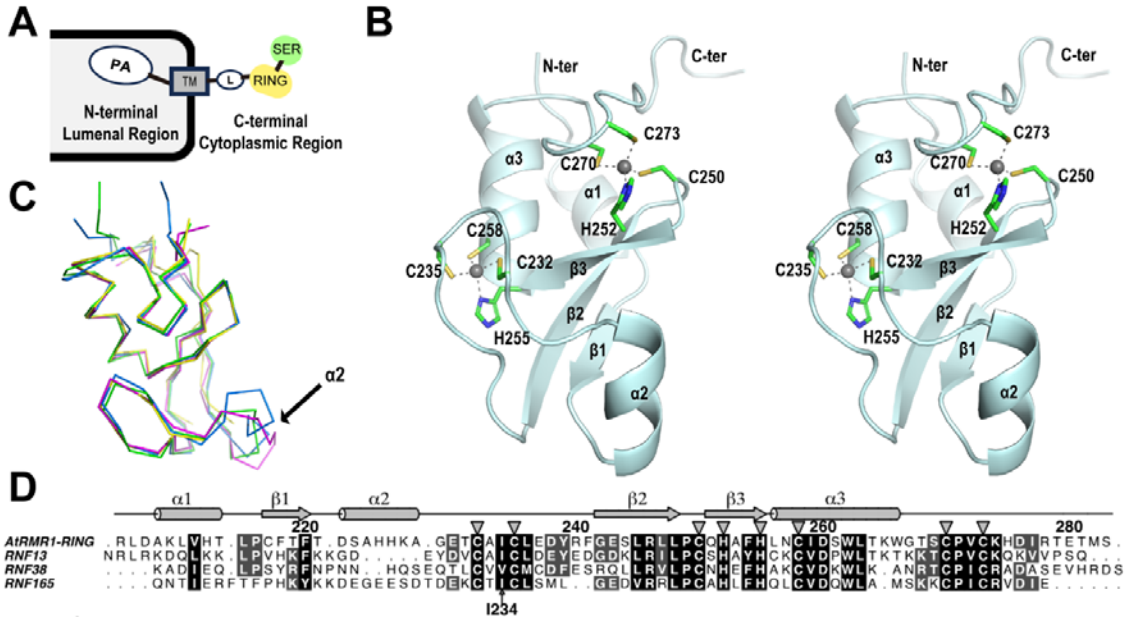

Figure 1. Crystal structure of AtRMR1-RING resembles an E3 ligase. (A) Domain organization of receptor-homology-transmembrane-RING-H2 (RMR) sorting receptors. RMR contains a protease-associated (PA) domain at its N-terminal lumenal region for cargo-binding. The C-terminal cytoplasmic region of RMR contains a RING-H2 (RING) domain connected to the transmembrane domain (TMD) via a Linker (L) domain, and a serine-rich (SER) domain. (B) Ribbon representations of the crystal structure of the RING-H2 domain of *Arabidopsis* RMR isoform-1 (AtRMR1-RING). The conserved C3H2C3 motif (Cys232, Cys235, Cys250, His252, His255, Cys258, Cys270 and Cys273) coordinating two Zn ions (grey spheres) is shown. Secondary structures of AtRMR1-RING are also labeled. (C) The structure of AtRMR1-RING (blue) is superimposable with the crystal structures of RNF13 (green, PDB code: 5ZBU), RNF38 (magenta, PDB code: 4V3K) and RNF165 (yellow, PDB code: 5D0M). Helix-2 of AtRMR1-RING is not conserved in other RING-H2 domains. (D) Sequence alignment of AtRMR1 with RNF13, RNF38 and RNF165. AtRMR1-RING shares 42%, 31% and 34% sequence identity to the RING-H2 domain of RNF13, RNF38 and RNF165, respectively.

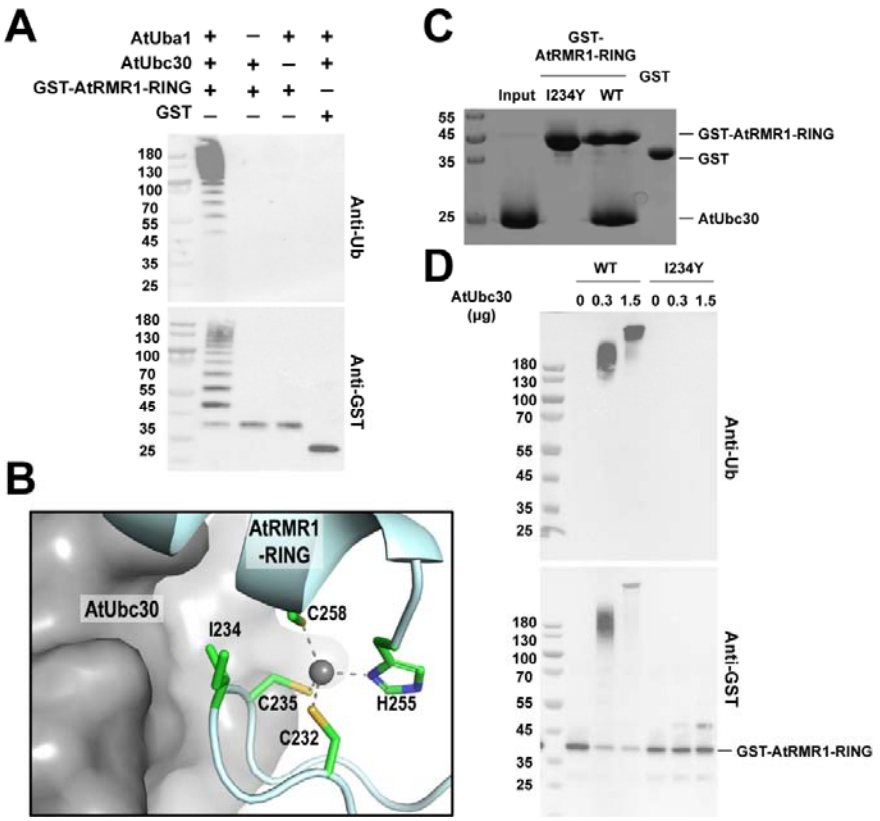

Figure 2. I234Y substitution disturbed the E3 ligase activity of AtRMR1-RING. (A) *In vitro* ubiquitination assay showing AtRMR1-RING is an E3 ligase. 1 µg GST-tagged AtRMR1-RING or GST were mixed with 0.1 µg Arabidopsis E1 ubiquitin-activating enzyme (AtUba1), 0.3 µg E2 ubiquitin-conjugating enzyme (AtUbc30), 2.5 µg ubiquitin (AtUb) in the presence of Mg^{2+} and ATP at 30 °C, 30 min and analyzed by Western blotting using ubiquitin (FK2, Enzo Life Sciences) and GST (Abcam) antibodies. (B) How AtRMR1-RING (cyan) interacts with AtUbc30 (grey) was predicted by homology modelling based on the crystal structures of the human RNF38/UbcH5B/Ubiquitin complex (PDB code: 4V3K). The conserved Ile234 of AtRMR1-RING is located at the interface between AtRMR1-RING and AtUbc30. (C) I234Y substitution disturbed the interaction between AtRMR1-RING and AtUbc30. 50 µM purified AtUbc30 (Input) was mixed with 50 µM wild-type, I234Y variant of GST-AtRMR1-RING or GST in the presence of GSTrap Sepharose (GE Healthcare). After extensive washing, bound proteins were eluted with 20 mM reduced glutathione and analyzed by 15% SDS-PAGE with Coomassie blue staining. AtUbc30 was co-eluted with wild-type GST-AtRMR1-RING but not with the I234Y variant nor the GST control. (D) I234Y substitution greatly reduced the E3 ligase activity of AtRMR1-RING. Wild-

type or I234Y variant of GST-AtRMR1-RING (1 µg) was incubated with AtUba1 (0.1 µg), AtUbc30 (0 µg, 0.3 µg or 1.5 µg) and AtUb (2.5 µg) in the presence of Mg^{2+} and ATP at 30 °C, 30 min. Poly-ubiquitination was detected by Western blotting using ubiquitin and GST antibodies. Poly-ubiquitination was evident in wild-type GST-AtRMR1-RING, but not in the I234Y variant, suggesting that I234Y substitution greatly reduced the E3 ligase activity.

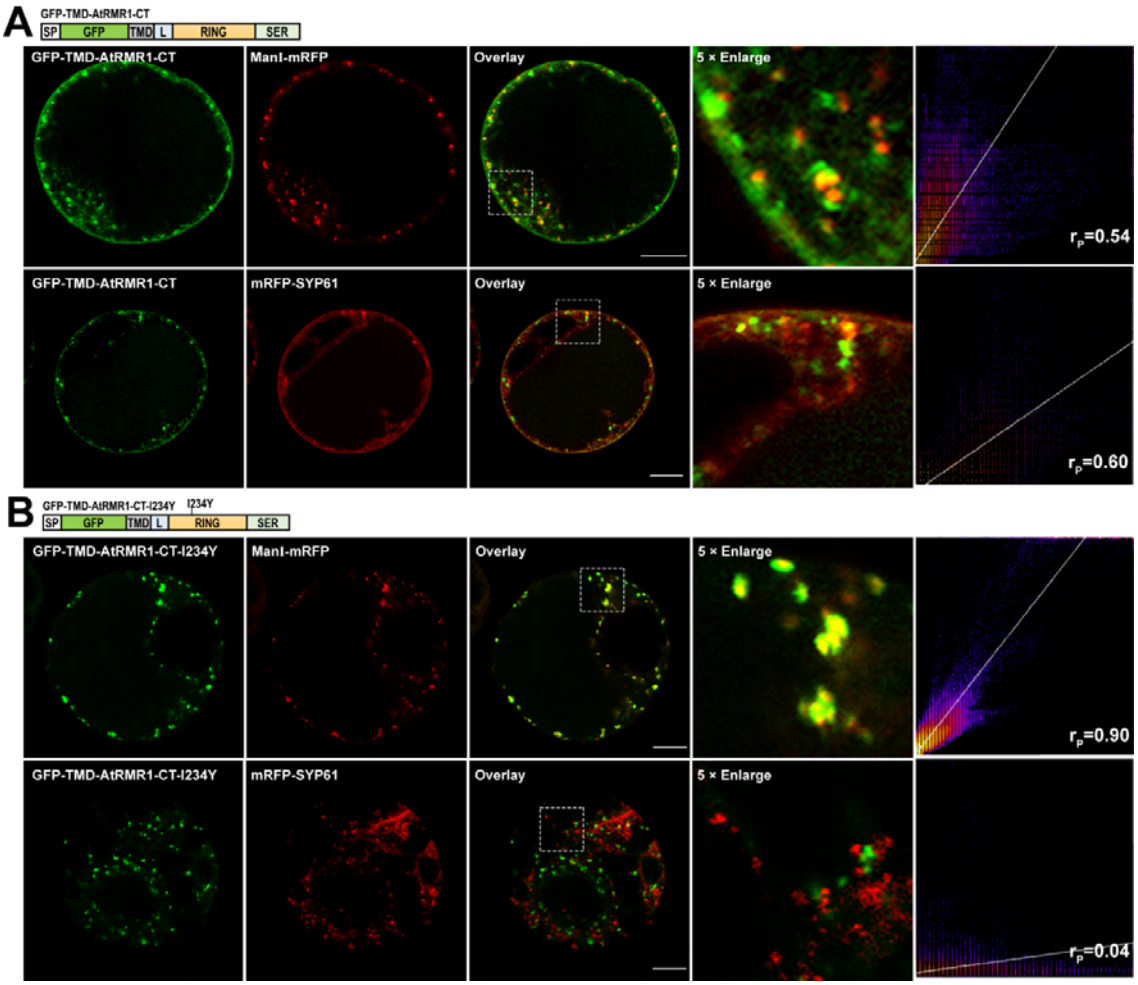

Figure 3. I234Y substitution resulted in Golgi retention of GFP-TMD-AtRMR1-CT in *Arabidopsis* protoplasts. *Arabidopsis* protoplasts were transfected with (A) wild-type or (B) I234Y mutant of GFP-TMD-AtRMR1-CT with the Golgi (ManI-mRFP) or TGN (mRFP-SYP61) markers before confocal imaging of transfected cells. The right column shows the scatterplot images obtained from FIJI with the Coloc2 co-localization plug-in. The extent of colocalization was quantified by linear Pearson correlation coefficient (r_P). (Scale bar,10 μm).

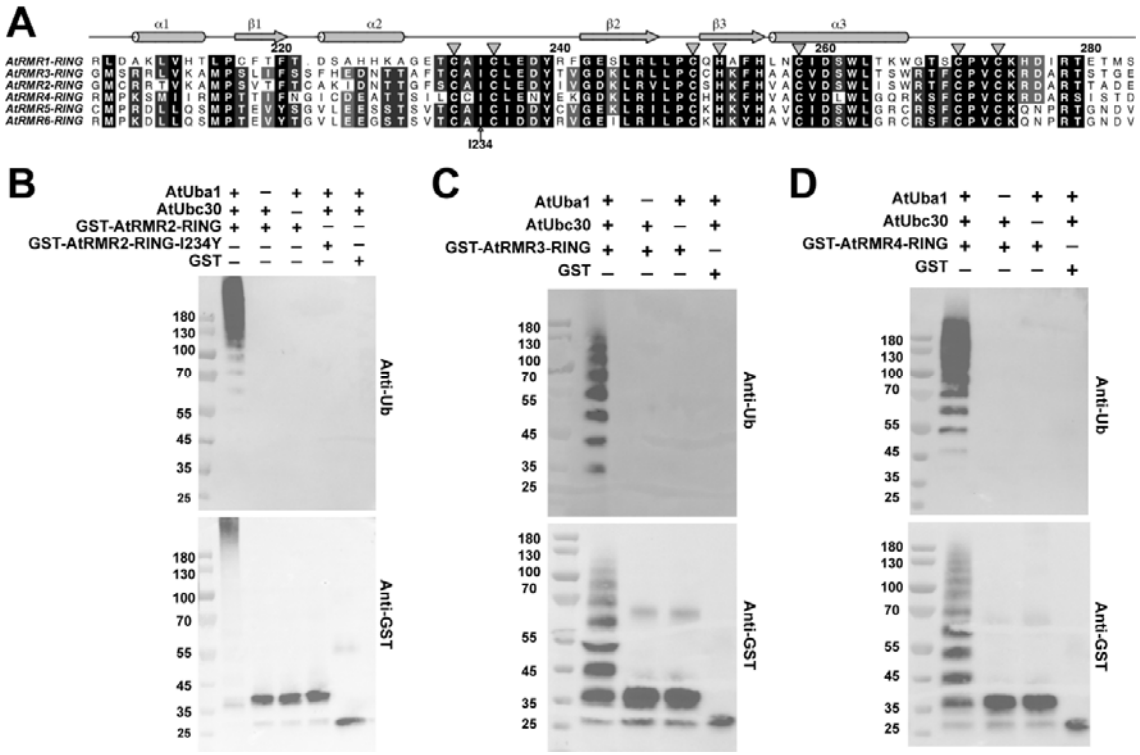

Figure 4. The RING domains of AtRMR2-4 are E3 ligases. (A) Sequence alignment of the RING domains of AtRMR1-6, showing conservation of the C3H2C3 motif (indicated by triangles) and Ile234 in AtRMR. (B) I234Y substitution disrupted E3 ligase activity of AtRMR2-RING. In the E3 ligase activity assay, GST, GST-tagged AtRMR2-RING, or its I234Y variant were mixed with Arabidopsis E1 ubiquitin-activating enzyme (AtUba1), E2 ubiquitin-conjugating enzyme (AtUbc30), and ubiquitin in the presence of Mg^{2+} and ATP at 30°C, 30 min and analyzed by Western blotting using ubiquitin (FK2, Enzo Life Sciences) and GST (Abcam) antibodies. In the presence of both E1 and E2, poly-ubiquitination was evident in wild-type GST-AtRMR2-RING but not in the I234Y variant. (C & D) The E3 ligase assay was performed for GST-tagged AtRMR3-RING or AtRMR4-RING. In the presence of both E1 and E2, poly-ubiquitination was observed for GST-AtRMR3-RING and GST-AtRMR4-RING.

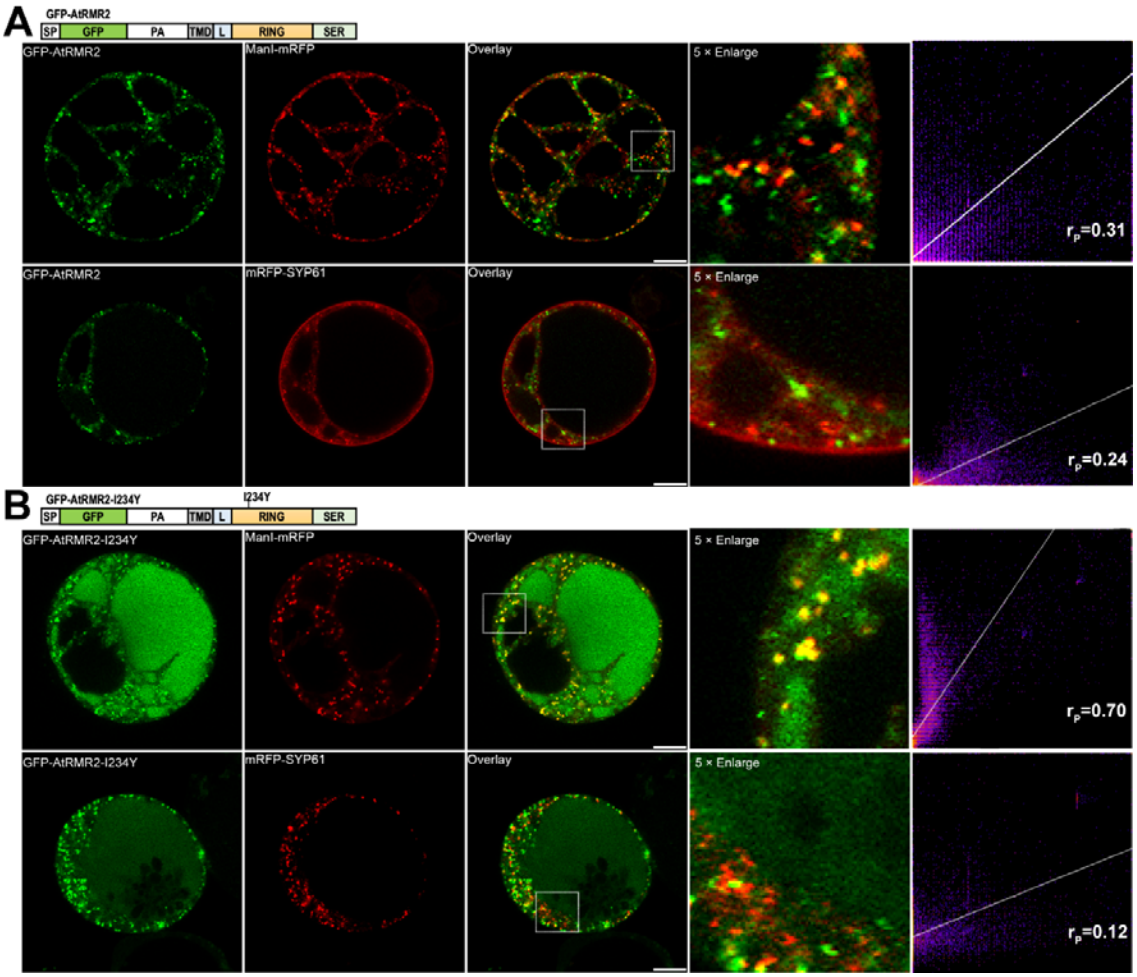

Figure 5. I234Y substitution resulted in Golgi retention of GFP-AtRMR2 in *Arabidopsis* protoplasts. *Arabidopsis* protoplasts were transfected with (A) wild-type or (B) I234Y mutant of GFP-AtRMR2 with the Golgi (ManI-mRFP) or TGN (mRFP-SYP61) markers before confocal imaging of transfected cells. The right column shows the scatterplot images obtained from FIJI with the Coloc2 co-localization plug-in. The extent of colocalization was quantified by linear Pearson correlation coefficient (r_P). (Scale bar,10 µm).